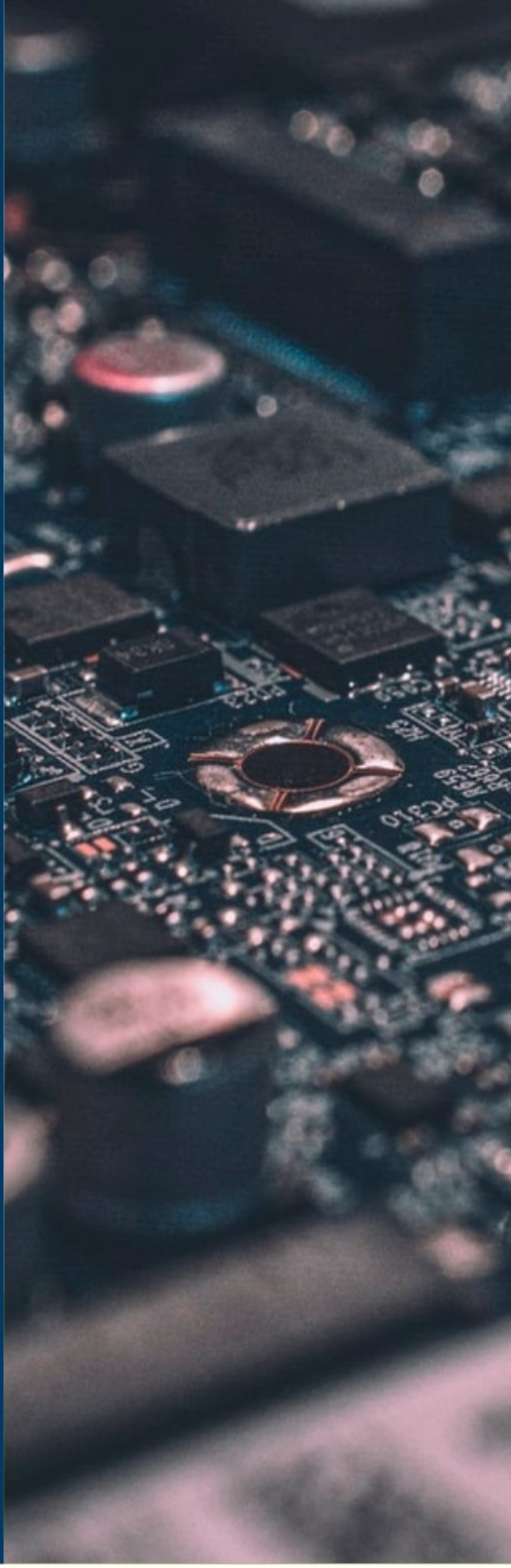

Performance enhancement of dual-band antenna for internet of things applications using closed loops

M. Kim, L. Qu, H. Shin and H. Kim✉

In this Letter, a dual-band antenna with improved performance is proposed by generating a stronger coupling with the ground plane using two closed loops. The antenna is designed in such a way that it is coupled with two orthogonal ground modes in the lower and higher bands. Two closed loops are attached at the end of the ground plane to control the frequencies of the two ground characteristic modes. Through simulation and experimental verification, the proposed antenna has obtained greatly improved performance in both bands compared to the reference antenna without closed loops.

Introduction: In recent years, researches on electrically small antennas (ESAs) for mobile devices have drawn great attention. It has been demonstrated that terminal antennas are necessarily coupled with the ground characteristic modes of the PCB to ensure good radiation [1–3] to counterbalance the fundamental limit of ESA [4]. However, due to the rapid development of the internet of things (IoTs) market, the overall sizes of IoT devices have become much smaller, limiting their capability to support high radiation performance of ESA. To reconcile this deficit, the so-called ground mode tuning (GMT) technique has been proposed to optimise the characteristics of the ground modes to obtain multi-functional performance. Optimisation can be achieved by tuning the resonant frequency of the ground plane nearly equal to that of the operating frequency [5–9]. With utilisation of the GMT technique, both the impedance bandwidth and radiation efficiency of the terminal antenna, which are key figures-of-merit for mobile antennas, can be greatly improved. Closed-loop structures such as the GMT technique [5] are advantageous in terms of convenience and low cost because they can be easily printed on the PCB without additional metal rims [6–9]. Until now, GMT has been widely used in performance improvement of the single-band antennas [5–7], implementation of MIMO antennas [8], and fabrication of a CP antenna [9]. However, simultaneous enhancement of antenna performance in both dual operating bands using GMT has remained challenging and has not yet been studied. This is especially true when miniaturised multiband antennas are required in small-sized IoT devices. For this purpose, it is essential to design a dual-band antenna where each operating band is independently coupled with two orthogonal ground modes since one GMT structure controls only one ground mode.

In this study, we focus on a dual-band antenna used in the applications of GPS for location tracking and Bluetooth for device connection. Therefore, we propose a high-performance dual-band antenna operating in the 1.575 GHz GPS band and the 2.45 GHz Bluetooth band, as a case study. These operation bands can be easily controlled by lumped elements of the antenna and GMT structures without modifying the antenna structure. The antenna elements are composed of two resonators coupling with different ground modes and two feeding loops controlling input impedances of the radiation elements independently. Two closed-loop GMT structures are inserted at the bottom and right sides of the ground plane to control, respectively, the resonant frequencies of the dominant ground mode along the *z*-axis (mode 1) and *y*-axis (mode 2), to improve radiation performance in the GPS band and Bluetooth band, respectively.

Antenna design and operating mechanisms: Fig. 1 illustrates the configuration of the proposed design. The proposed dual-band antenna consists of a monopole-type resonator for the lower band, loop-type resonator for the higher band, and a feed structure. The monopole-type resonator is composed of a vertical conductor inside the clearance, an inductor L_{RL}, a horizontal conductor at the left-side of the clearance, and a meandering structure vertically set at the top of the ground plane. The loop-type resonator is comprised of a vertical conductor inside the clearance and a horizontal conductor at the right-side of the clearance as well as a capacitor C_{RH}. It is noted that the two resonators are designed in such a way that they can excite the ground mode 1 and ground mode 2, respectively for far-field radiation. Accordingly, the resonance frequencies of two radiating elements can be controlled by adjusting the value of the inductor L_{RL} and the value of the capacitor C_{RH}, respectively. Moreover, two feeding loops are printed on the bottom plane of the PCB. The left-side loop excites the monopole-type resonator, while the right-side loop excites the loop-type resonator; the impedance matching of both resonators can be controlled by adjusting the values of C_{FL} and C_{FH}, respectively.

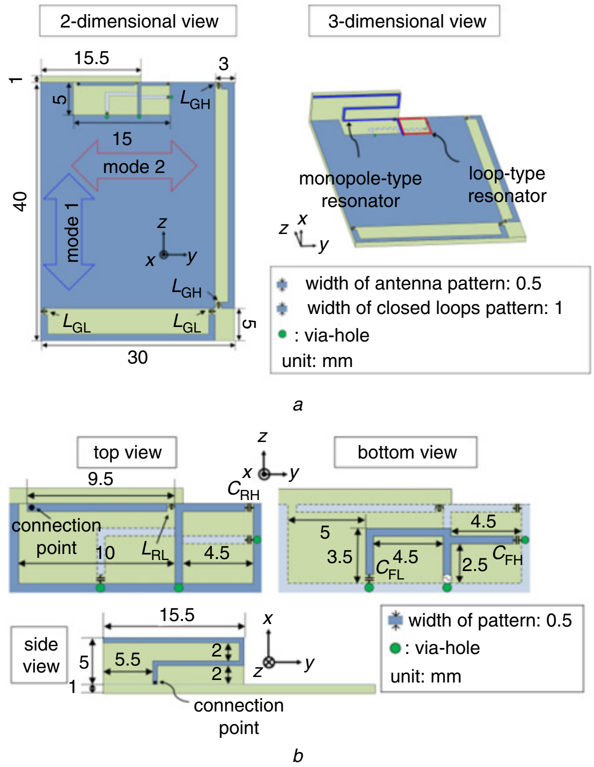

Fig. 1 *Configuration of the proposed design*
a Overview
b Antenna elements

To improve the radiation performance at both operating bands, two closed loops are inserted at the bottom- and right-sides of the ground plane as GMT technique. As can be observed in Fig. 1, the closed loop at the bottom side is constructed within a dimension of 5 mm × 27 mm and is terminated by inductors L_{GL} (15 nH) so that it can effectively control the resonance of the ground mode 1. The closed loop at the right side with a dimension of 3 mm × 35 mm is terminated by inductors L_{GH} (2.5 nH) so that it can be utilised to effectively control the resonance of the ground mode 2.

The performance of the antenna can be dramatically improved by controlling each mode to resonate at the operating frequency, as shown below. As a comparison, the reference design is designated as the antenna design with the full ground without closed loops. The optimised values of C_{FL}, C_{FH}, L_{RL}, C_{RH} are set as 1.1pF, 0.175 pF, 3.2 nH and 0.325 pF, respectively, for the reference design and 1.5 pF, 0.25 pF, 3 nH and 0.3 pF, respectively, for the proposed design.

Fig. 2 shows the surface current distributions of the reference and proposed designs in both bands. In the low band (1.575-GHz GPS band), the monopole-type resonator is located at the *E*-field maximum portion of the ground mode 1 and more vertical currents are induced to the ground plane with the utilisation of the bottom-side closed loop, indicating its radiation performance is greatly improved. Further, high current distribution is generated into the bottom-side closed loop, demonstrating its effectiveness in controlling the ground mode 1. In the high band (2.4 GHz Bluetooth band), the loop-type resonator is located at the *H*-field maximum of the ground mode 2, thereby generating a strong coupling with ground mode 2 for far-field radiation. With the introduction of the right-side closed loop, more horizontal current distributions are induced to both the closed loop and the ground plane, indicating the suitability of the closed loop and improved radiation performance at the higher band.

Fig. 3 shows the simulated reflection coefficients of the reference and proposed designs. In the low band (1.575-GHz GPS band), the simulated 3:1 voltage standing wave ratio (VSWR) impedance bandwidth was 60 MHz (from 1544 to 1604 MHz) for the reference design and improved up to 180 MHz (from 1528 to 1708 MHz) for the proposed design. In the high band (2.4 GHz Bluetooth band), the simulated 3:1 VSWR impedance bandwidth was 85 MHz (from 2396 to 2481 MHz) for the reference design and improved up to 284 MHz (from 2285 to 2569 MHz) for the proposed design. Fig. 4 shows the impedance of the reference and proposed designs on Smith charts. It can be observed that a parasitic locus (ground mode 1) is generated at the lower frequency band, and its resonant frequency can be lowered by increasing the value of L_{GL}. Therefore, a dual-resonance characteristic is generated for optimised performance at the lower band when $L_{GL} = 15$ nH. Similarly, another parasitic locus (ground mode 2) is excited so that dual-resonance and wideband properties are produced when $L_{GH} = 2.5$ nH.

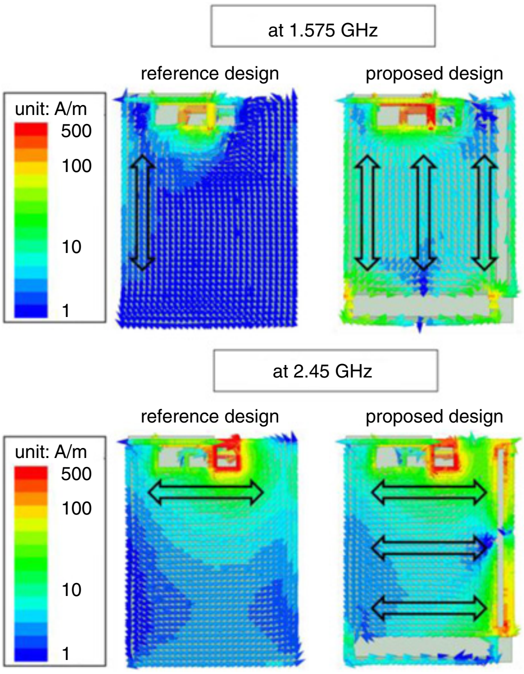

Fig. 2 *Simulated surface current distributions in both bands*

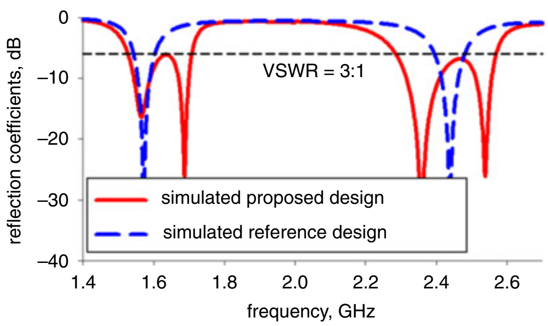

Fig. 3 *Simulated reflection coefficients*

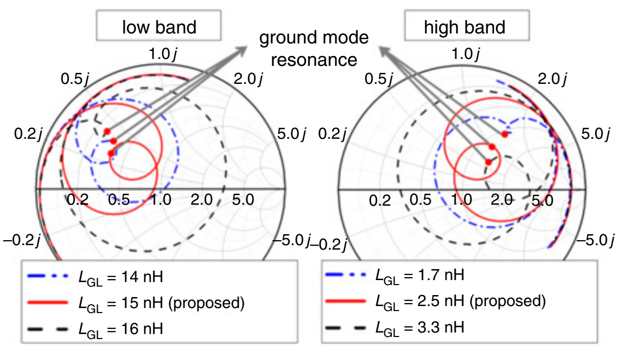

Fig. 4 *Simulated input impedance on Smith charts*

Experimental results: Fig. 5 presents the measured reflection coefficients and total efficiencies of the reference and proposed designs. In the low band (1.575 GHz GPS band), the measured 3:1 VSWR impedance bandwidth was 105 MHz (from 1511 to 1616 MHz) for the reference design and improved up to 187 MHz (from 1507 to 1694 MHz) for the proposed design. In the high band (2.4 GHz Bluetooth band), the measured 3:1 VSWR impedance bandwidth was 108 MHz (from 2407 to 2515 MHz) for the reference design and improved up to 295 MHz (from 2294 to 2589 MHz) for the proposed design. It can be verified that the simulation and measurement agree with each other, indicating that the proposed method can be utilised to greatly improve the impedance bandwidth of the dual-band antenna. The total efficiency at 1.575 GHz improved from 44 to 67% by utilising the bottom-side closed loop. In the higher band, the reference and proposed antennas generate an average efficiency of 41 and 70%, respectively. Fig. 6 shows the measured radiation patterns of the proposed design in lower and higher bands. The proposed antenna produces omni-directional radiation patterns on the *xy*-plane in the lower band and on the *xz*-plane in the higher band, indicating that the bands excite ground mode 1 and ground mode 2, respectively, for far-field radiation.

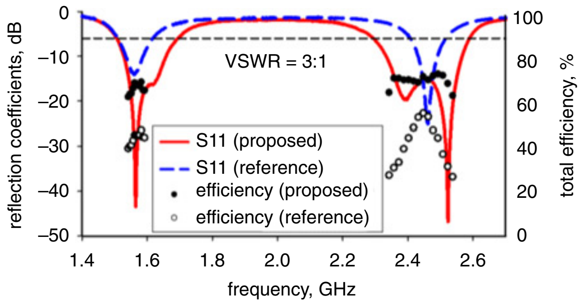

Fig. 5 *Measured reflection coefficients and total efficiencies of the reference and proposed designs*

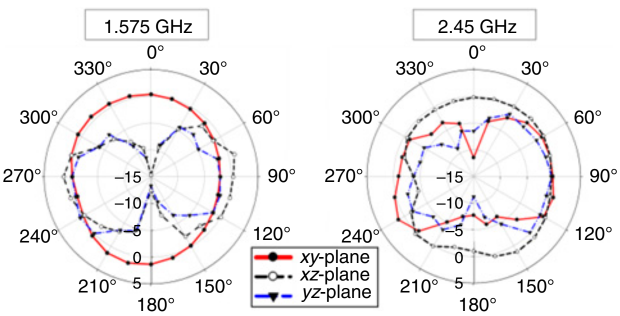

Fig. 6 *Measured radiation patterns of the proposed antenna*

Conclusion: This letter presented an effective method to improve the radiation performance of a dual-band antenna on a small ground plane by controlling the ground modes. The antenna element was designed to ensure a strong coupling with two orthogonal ground modes in both bands. Two closed-loop structures were inserted as the GMT technique to control both the vertical ground mode (ground mode 1) and the horizontal mode (ground mode 2), thereby improving the antenna performance at each band. In the proposed design, the 3:1 VSWR impedance bandwidth was three times higher in the low band and 3.34 times higher in the high band than in the reference design, and the measured total efficiency was 1.5 times higher in the low band and 1.7 times higher in the high band. By observing the measured radiation patterns, it was verified that the proposed antenna generates a dipole-type radiation pattern along the *z*-axis at the lower band and along the *y*-axis at the higher band.

Acknowledgment: This work was supported by a grant from the National Research Foundation of Korea (NRF), funded by the Korean government (MSIT) (no. 2019R1F1A1063993).

Submitted: *05 July 2019* E-first: *21 October 2019*
doi: 10.1049/el.2019.2278
One or more of the Figures in this Letter are available in colour online.

M. Kim, L. Qu, H. Shin and H. Kim (*Department of Electronics and Computer Engineering, Hanyang University, Seoul, Republic of Korea*)

✉ E-mail: hdkim@hanyang.ac.kr

References

1 Fallahpour, M., and Zoughi, R.: 'Antenna miniaturization techniques: A review of topology-and material-based methods', *Antennas Propag. Mag.*, 2017, **60**, (1), pp. 38–50

2 Villanen, J., Ollikainen, J., Kivekas, O., *et al.*: 'Coupling element based mobile terminal antenna structures', *Trans. Antennas Propag.*, 2006, **54**, (7), pp. 2142–2153

3 Zahid, Z., and Kim, H.: 'Analysis of a loop type ground radiation antenna based on equivalent circuit model', *Microw. Antennas Propag.*, 2017, **11**, (1), pp. 23–28

4 McLean, J.S.: 'A re-examination of the fundamental limits on the radiation Q of electrically small antennas', *Trans. Antennas Propag.*, 1996, **44**, (5), pp. 672–676

5 Yoo, S., Qu, L., Kim, J., *et al.*: 'Mobile antenna performance improvement by ground mode tuning using a closed loop', *Microw. Antennas Propag.*, 2017, **11**, (8), pp. 1121–1126

6 Qu, L., Zhang, R., Shin, H., *et al.*: 'Performance enhancement of ground radiation antenna for Z-wave applications using tunable metal loads', *Electron. Lett.*, 2016, **52**, (22), pp. 1827–1828

7 Qu, L., Zhang, R., Shin, H., *et al.*: 'Mode-controlled wideband slot-fed ground radiation antenna utilizing metal loads for mobile applications', *Trans. Antennas Propag.*, 2017, **65**, (2), pp. 867–872

8 Qu, L., Lee, H., Shin, H., *et al.*: 'MIMO antennas using controlled orthogonal characteristic modes by metal rims', *Microw. Antennas Propag.*, 2017, **11**, (7), pp. 1009–1015

9 Qu, L., Zahid, Z., Kim, H.-H., *et al.*: 'Circular polarized ground radiation antenna for mobile applications', *Trans. Antennas Propag.*, 2018, **66**, (5), pp. 2655–2660